

Analysis of planetary waves seen in ionospheric total electron content (TEC) perturbations

P. Hoffmann, C. Jacobi

Zusammenfassung

Am DLR Neustrelitz wird kontinuierlich die totale Ionisation der Atmosphäre bestimmt und globale Karten der vertikal integrierten Elektronendichte erstellt. Es werden dazu die Signale der Navigationssatelliten-Systeme GPS und GLONASS verwendet. In dieser Arbeit wird die Verteilung des totalen Elektronengehalt (TEC) oberhalb der mittleren Breiten während der Übergangssaison September bis November 2004 auf langperiodische Variationen im Bereich von mehreren Tagen sowie zonalen Wellenzahlen bis zu 5 untersucht. Die Ergebnisse werden mit einer Analyse von planetaren Wellen aus assimilierten Stratosphärendaten, Radardaten für Temperatur vom Collm Observatorium (51.3°N, 13.0°O) und Beobachtungen der kritischen Plasmafrequenz der F2-Schicht (f_0F2) mit der Ionosonde in Juliusruh (54.6°N, 13.4°O) verglichen, um den meteorologischen Einfluss auf die Variation der Ionosphäre zu studieren.

Summary

The DLR Neustrelitz regularly produces maps of the total total electron content (TEC) on a global scale using the navigation satellite systems GPS and GLONASS to forecast space weather. In this study we turn our attention to the higher middle latitudes TEC variations during September to November 2004 in a long-period range of several days with a zonal wavenumber up to 5. The results are compared with a planetary wave analysis using assimilated stratospheric data, mesosphere/lower thermosphere radar temperature data at Collm observatory (51.3°N, 13.0°E) and the ionosonde observed critical plasma frequency of the F2-layer (f_0F2) at Juliusruh (54.6°N, 13.4°E) to investigate the meteorological influences on ionospheric variability.

1. Introduction

The ionosphere is the part of the upper atmosphere where free electrons are produced by ionisation of neutral atoms or molecules through solar X-rays and EUV radiation. The vertical structure of the neutral atmosphere depends on temperature and the vertical distribution of plasma density. In the ionospheric F-region (170 to 1000 km) the atomic oxygen is ionized during daytime. At night the recombination is not sufficient to neutralize the total layer. Electromagnetic waves passing the ionosphere are permanently modified by F-layer. This property allows to observe ionospheric variabilities.

The space weather monitoring controls extraterrestrially the variability of ionizing radiation with solar origin (solar rotation, solar flares). Using dual frequency global position system (GPS) measurement, the total electron content (TEC) of the ionosphere is de-

rived, and TEC maps in a hemispheric scale are created by DLR Neustrelitz (Jakowski et al, 2002). These hourly received ionospheric data are used to analyse signals from below in the complex vertically coupled atmospheric system.

The ionosphere is coupled to the lower atmosphere through upward propagating waves in the neutral atmosphere. These waves with quasi periods of 2 to 30 days are planetary wave types and deposit energy from below. Solar tides with periods of 12 h and 24 h are also relevant in this context. However, the main variations of the ionosphere are affected by electrical and electromagnetic phenomena (Lastovicka, 2005).

Planetary wave activities have already been indentified from ionosonde measurements by Forbes et al. (2000) and Altadill et. al. (2002). Lawrence (2003) analysed planetary waves from simultaneous observations in a range of 30 to 220 km based on different data sources from 10th April to 18th August (130 days) in 1997, 1998 and 1999. ECMWF reanalysis data (stratosphere), HF radar data (mesosphere) and the ionosonde frequencies (thermosphere) were used by these to detect planetary waves in the atmosphere. Signals of the quasi 10- and 16-day waves were found in all atmospheric layers.

2. Ionospheric variables

2.1 The total electron content

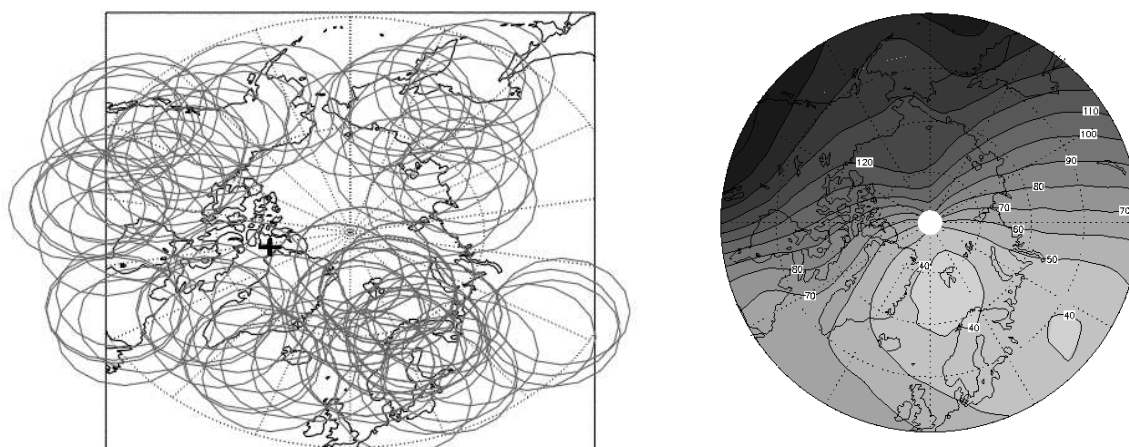


Figure 1: Data coverage of GPS based TEC monitoring during a selected snapshot on 5 Nov. 2001 at 2 UT over the northern Hemisphere (left panel), taken from <http://www.kn.nz.dlr.de/>. The vertical TEC values are computed for a grid of 567 points within the latitude range $50^{\circ}N \leq \phi \leq 90^{\circ}N$. The range of each measuring point is indicated by isolines of the half width of TEC Amplitude weighting functions. A produced TEC map at 23 September 2004 0 UTC over the northern hemisphere (right panel). The contour lines are plotted in TEC ($10^{16} m^{-2}$).

The TEC as a indicator of ionospheric variability is derived by the modified GPS signal through free electrons. The two coherent carrier frequencies of the L-band ($L_1=1.575$ GHz, $L_2=1.228$ GHz) are received by 30 ground stations. They measure the differential phase, $\Delta\Phi$, of the two waves and derives the TEC by a well approximated ionospheric refractive index (Kohl et al, 1996). Since 1995, TEC maps over the European sector are operationally generated, and global maps followed later. Figure 1 shows the northern hemispheric coverage with GPS-satellites at fixed time (left panel) and an example of a

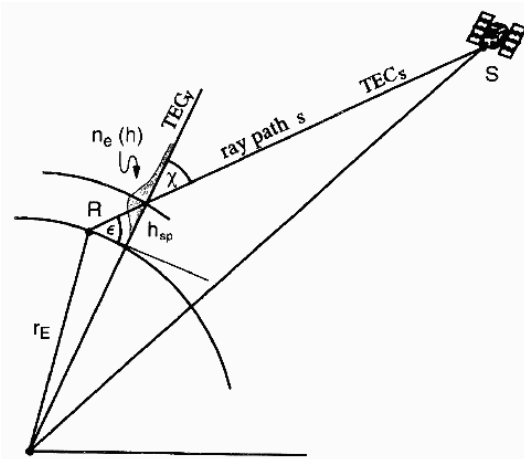


Figure 2: Ray path geometry for the trans-ionospheric satellite signals shows the derivation of the total electron content (TEC_v).

TEC map (right panel). The plot shows the distribution of total ionization over the mid-latitude region with a grid resolution of 7.5° longitude by 2.5° latitude. The vertical TEC profile has been validated by ionosondes and ionospheric radio occultation (IRO) GPS measurements on board the German geoscience satellite CHAMP at low earth orbit (LEO). The definition of the TEC value is given in Eq. (1). One TEC unit (TECU) corresponds to 10^{16} electrons per m^2 and is measured with an accuracy of better than $3 \cdot 10^{16} m^{-2}$. The transformation of the measured TEC values (TEC_s) along the ray path to the vertical TEC_v points the simple geometric relation in Figure 2. r_E is the Earth's radius and $n_e(h)$ the electron density dependent at height h :

$$TEC_s = \int n_e ds, \quad (1)$$

$$TEC_v = TEC_s \cdot \sqrt{1 - \left(\frac{h_{sp} \cos \epsilon}{h_{sp} + r_E} \right)^2}. \quad (2)$$

2.2 Modern ionosondes

Ionosondes detect the ionosphere's different layers and their activities. They have been used since a few decades. The station Juliusruh ($54.6^\circ N$, $13.4^\circ E$) in northern Germany measures the critical f_0F_2 -frequency parameter of an ionosonde since about 1960. Today, modern ionosondes are digital and work precisely. They measure signatures of reflected electromagnetic waves on ionospheric free electrons. The automatically scaled and multi-parameter ionogram provides ionospheric properties and electron density profiles in real time. The ionosonde generally scans from 1 to 20 MHz, transmitting modulated HF radio waves, and further receiving and analysing the ionospherically reflected echo signal. The transmitted radio waves with a frequency higher than the f_0F_2 -frequency pass the ionosphere. The TEC is derived from the given critical plasma frequency Eq. (3). The variables N_e , e and m are number density, charge and mass of the electron, ϵ_0 is the free space permittivity:

$$f_P = \sqrt{\frac{N_e \cdot e^2}{4\pi^2 m \epsilon_0}}. \quad (3)$$

3. Neutral atmospheric data

3.1 The UK Met Office reanalysed stratospheric data

The UK Met Office stratospheric data are analysed on 25 standard pressure levels from 1000 hPa to 0.1 hPa (approx. 0 to 55 km) on a 2.5° latitude by 3.75° longitude global grid. They are produced by assimilating operational meteorological observations daily at 12 UTC, including data from NOAA polar orbiters. The data assimilation system used is produced by the Met Office for operational weather forecasting. Further details are given

in Swinbank and O'Neill (1994) and Lorenc et al. (2000).

Table 1 taken from the UK Met Office stratospheric analyses documentation gives the quality of the assimilated data. In general, the errors are higher than average at high latitudes and during winter. In particular, errors will be larger (perhaps 10 to 20 K locally) during dynamically active periods such as stratospheric warmings, near the poles, and equator and also larger near the tropopause (200 to 300 hPa at mid-latitudes).

Pressure-level	Velocity	Geopotential Height	Temperature
1000 hPa	6.0 m/s	10 m	1.0 K
tropopause	9.0 m/s		1.5 K
100 hPa	6.0 m/s	20 m	1.0 K
10 hPa	8.0 m/s	70 m	1.0 K
1 hPa	12.0 m/s	100 m	2.0 K

Table 1: *Estimated RMS error as an indicator for the assimilated data quality. (<http://badc.nerc.ac.uk/data/assim/documents.html>, visited on December 2005)*

3.2 Meteor radar at Collm Observatory (51.3°N, 13.0°E)

The measurements deliver hourly wind information in the height range 80 to 100 km and daily mean temperature near the mesopause. The ground based instrument using LF radio waves of 32.6 MHz frequency (6 kW peak) with pulses of 13 μ s length and 2144 Hz repetition frequency. The calculated wind is derived by the Doppler shift of reflected radio waves from ionized meteor trails. The temperature measurement is determined by the diffusion coefficient and an empirical temperature gradient model (Hocking et al., 1999). Specific details of the radar and a data analysis of autumn 2004 is given by Jacobi et al. (2005).

4. Planetary wave analysis

The planetary waves at mid-latitudes are generally Rossby waves with a zonal wavenumber of 1,2 or 3 and quasi-periods of 5, 10 and 16 days. They are forced in the troposphere by topography, land–sea temperature contrasts as well as synoptic eddies, and they propagate horizontal and vertical directions. Planetary waves can be detected, for example, by analysing atmospheric temperature.

A discrete Fourier analysis (Eq. 5), decomposes the variations in a time series $f(t)$, into harmonic functions, and thereby transforms the information into the frequency domain. Similarly the spatial variations along one longitude $f(x)$ can be analysed (Eq. 6). The spectral distribution of the amplitudes (A_k , A_ω) and phases (ϕ_k , ϕ_ω) indicates waves with characteristic frequencies (or periods), f_k , and zonal wavenumbers, k :

$$f_k = \frac{\omega_k}{2\pi} = \frac{2\pi}{T} = \frac{k}{n}. \quad (4)$$

The temporal and spatial Fourier decomposition is given by:

$$f(x, t) = a_0(x) + \sum_{\omega} c_{\omega}(x) \cos(\omega t) + s_{\omega}(x) \sin(\omega t), \quad (5)$$

$$f(x, t) = b_0(t) + \sum_k c_k(t) \cos(kx) + s_k(t) \sin(kx). \quad (6)$$

The amplitude and phase is calculated as follow:

$$A = |\sqrt{c^2 + s^2}|, \quad \phi = \tan^{-1} \left(\frac{s}{c} \right). \quad (7)$$

5. Results

The atmospheric data analysis is carried out for different data sources listed in Table 2. The main task is to find characteristically planetary waves at different height, detected by ionosonde and meteor radar as well as by analyzed assimilated data from stratosphere and TEC maps.

	GNSS	REANALYSES	RADAR	IONOSONDE
Variables	TEC	U, V, H, T	U, V, T	f ₀ F2
Longitude	0° ≤ λ ≤ 360°	0° ≤ λ ≤ 360°	13.0°E	13.4°E
Latitude	50°N ≤ φ ≤ 90°N	90°S ≤ φ ≤ 90°N	51.3°N	54.6°N
Grid Solution	λ=7.5°, φ=2.5°	λ=3.75°, φ=2.5°		
Height	200 - 300 km	10 - 60 km	~ 90 km	~ 250 km
Time Solution	hourly	daily	daily	hourly

Table 2: Overview on used atmospheric data.

5.1 Seasonal upper atmosphere climatology based on CIRA 86

First the seasonal variation of temperature and zonal wind up to 120 km height are described (Figure 4). Between summer and winter there is a marked difference in height–latitude cross section of the zonal wind at upper atmospheric level. The stratosphere and mesosphere up to 90 km height are characterized by an eastward directed

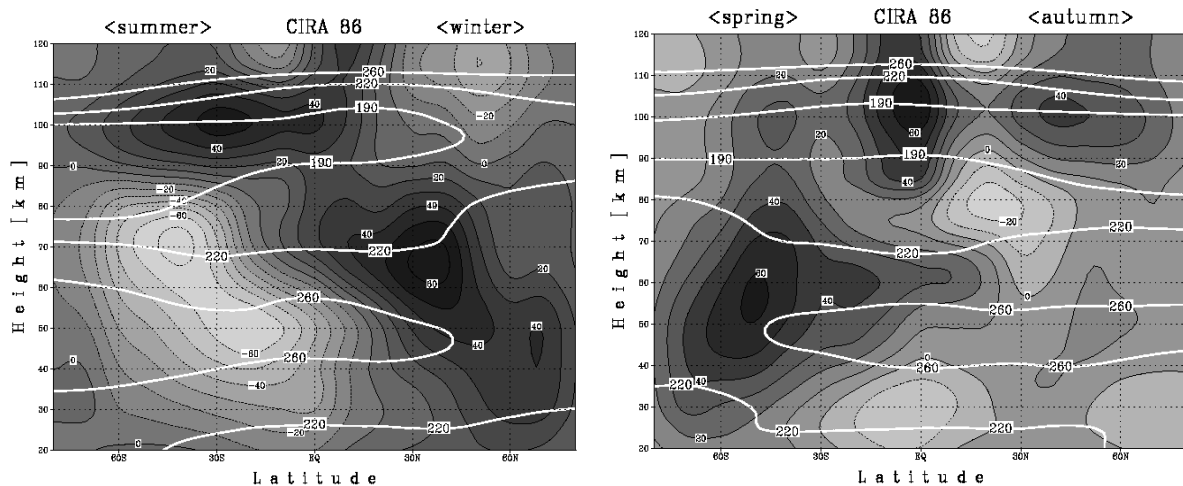


Figure 3: Monthly mean temperature (solid white) and zonal wind speed (shaded) data from CIRA 86 (COSPAR International Reference Atmosphere). The summer middle atmosphere condition is characterized by the southern hemisphere during January and the winter season by the northern hemisphere (left panel). The autumn and spring conditions (right panel) are shown by the April mean. Negative speed values mean eastward and positive values westward directed wind speed.

jet in summer and a westward directed jet in winter season (left panel, shaded). Above mesopause region changes the direction to west in summer and east in winter. During the spring and autumn months, the upper atmosphere conditions are more variable. The differences of the dynamic regimes between summer and winter are inverted (right panel). The temperature conditions (solid white lines) show a colder mesopause in summer (~ 170 K) than in winter (~ 200 K). The stratopause temperature is near 260 K.

5.2 Stratospheric condition during autumn 2004

During the autumn months September to November the upper atmosphere below the mesopause region changes from northern hemispheric summer (eastward directed jet) to winter (westward directed jet) conditions. Figure 5 depicts the monthly mean September

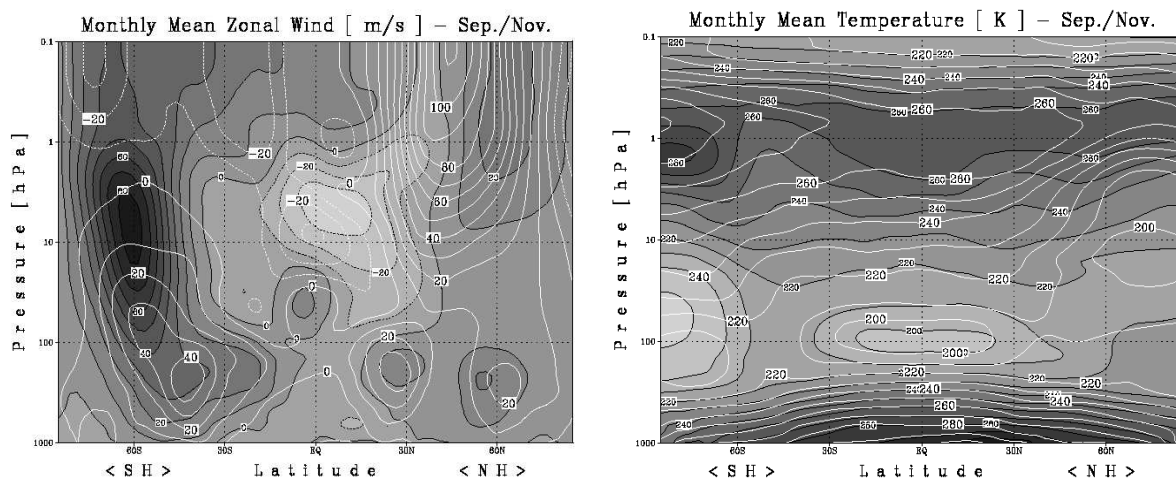


Figure 4: The monthly mean zonal wind (left panel) for September (shaded) and November (white solid) 2004 are shown together with the monthly mean temperature (right panel) for September (shaded) and November (white solid) at 0° E.

2004 (shaded) for zonal wind (left panel) and temperature (right panel). In height-latitude cross section plots are overlaid the november conditions (white solid lines). Table 3 summarizes the main differences in temperature and zonal velocity at 1.0 hPa height and $60^\circ\text{N}/60^\circ\text{S}$ for monthly mean conditions in September and November 2004. The temperature decreases from about 280 K to 250 K and the monthly mean zonal speed rises starting with 20 m/s in September and ending with 60 m/s in November.

Hemisphere	Zonal Wind (Sep/Nov)	Temperature (Sep/Nov)
Northern	(20/60) m/s	(280/250) K
Southern	(50/-10) m/s	(260/270) K

Table 3: Approximated comparison of the atmospheric conditions at 1.0 hPa height and at latitude 60° on the northern and southern hemisphere between September and November 2004.

5.3 Time series

The analysis of planetary waves is carried out in the time range from 1st September to 20th November 2004. Figure 5 shows the time series at mid-latitude regions near 55°N and 15°E for the hourly TEC values and ionosonde data (f_0F2) at Juliusruh (54.6°N ,

13.4°E) as well as the daily mean meteor radar temperature at Collm (51.3°N, 13.0°E) and the assimilated temperature data from UK Met Office data centre at 1.0 hPa height.

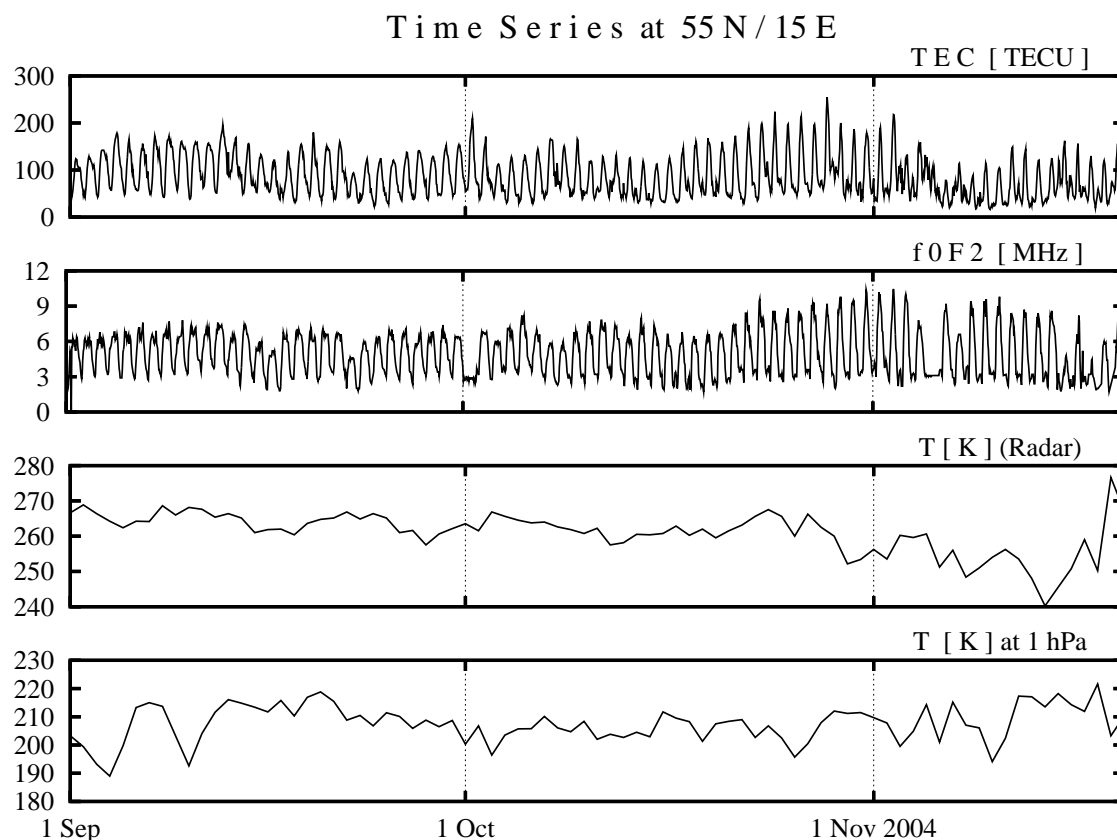


Figure 5: Time series starting on 1st September and ending on 20th November 2004. Hourly values for TEC and Ionosonde data, daily mean values for the radar and Met Office data. The global data TEC and Met Office are taken at 55.0° N and 15.0° E.

5.4 Spectral analysis

The Fourier analyzed time series are shown in Figure 6. The resulting amplitude spectra separate dominant variations in a range of periods from 2 to 30 days. For every time series one receives an characteristically spectrum with marked periods. In all spectra there are oscillations of quasi 6 and 30 days. The 10-day wave is not detected in temperature data at 1 hPa, and in TEC data is the 16-days wave missing. All results are summarized in Table 4. In a range near one day and shorter one can find the solar tides of periods about 24 h, 12 h and 8 h in case of hourly data.

5.5 30-day running window spectra

The Fourier analysis of a 30-days running window (shifted by one day) is depicted in Figure 7. The resulting structures show the wave activities for characteristic periods of days at different times between September and November. The 10-day wave is very dominant especially in ionospheric data. Longer periodic variation (> 15 d) cannot be resolved because of the limited window length.

Periods $\pm 1d$	TEC	T at 1.0 hPa	T (Radar)	f_0F2
6 d	y	y	y	y
10 d	y	n	y	y
12 d	y	y	n	n
16 d	n	y	y	y
30 d	y	y	y	y

Table 4: Summarized results of spectral analysis. Is there a marked peak in the given range of the selected period, than 'y' else 'n'.

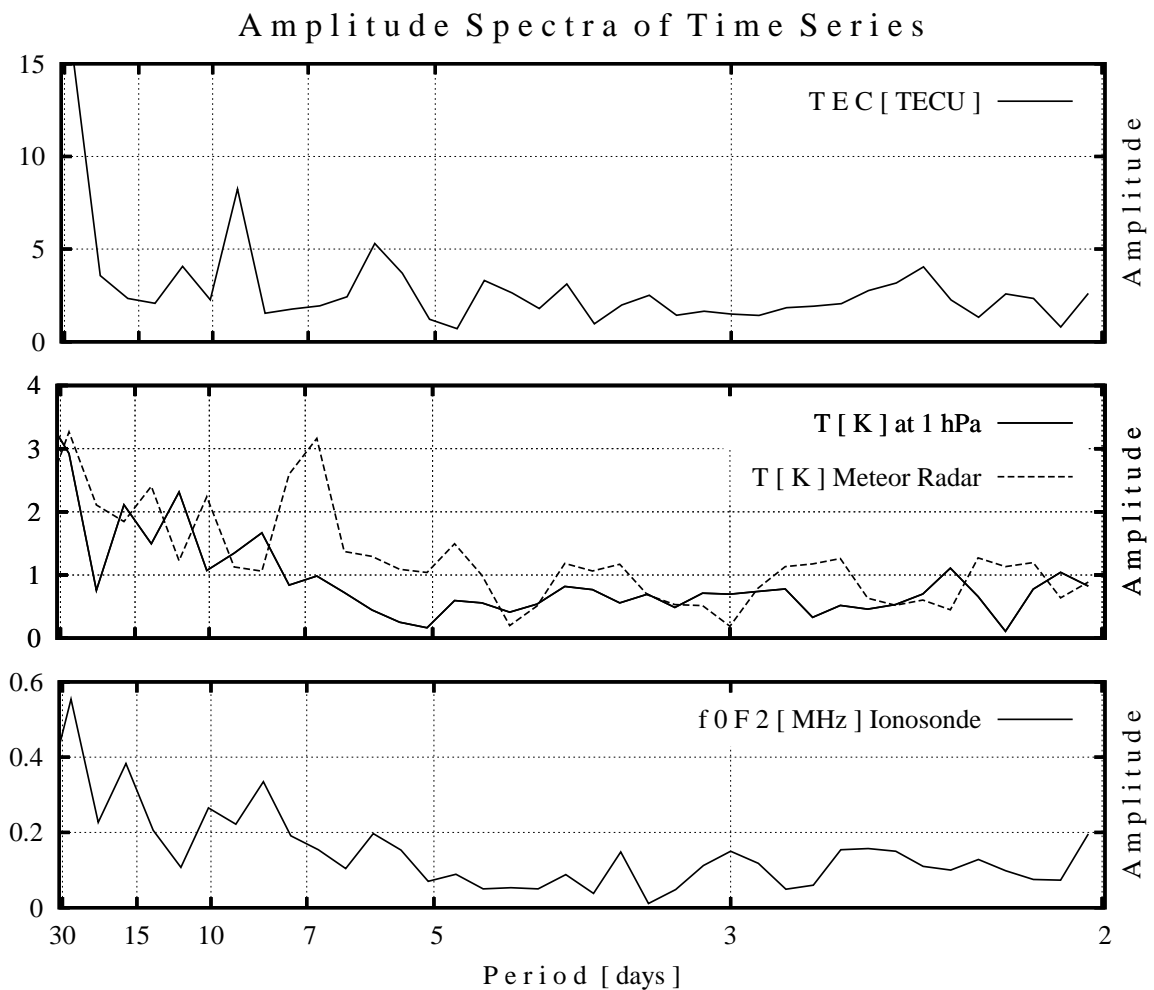


Figure 6: Plotted amplitudes of the Fourier analyzed data from TEC data, ionosonde (f_0F2), temperature from meteor radar and UK Met Office temperature (1.0 hPa), all at about $55^\circ N$ and $15^\circ E$.

5.6 Zonal wavenumber analysis

Beneath the analysis of variations in time the global TEC data and UK Met Office data allows an harmonic analysis in spatial variations. One receives amplitude and phase for the zonal wavenumbers 1, 2, 3. Figure 8 shows the results of the zonal analysis of TEC and temperature at 1.0 hPh. As expected, the amplitude of zonal wavenumber 1 dominates. At the end of October the amplitudes for wavenumber 2 and 3 become more important. The changing of phase in time describes how waves propagate. For example, the phase of $k=1$ in TEC data does not vary in time. This wave is of quasi stationary type.

30-Days Running Window Amplitude Spectra

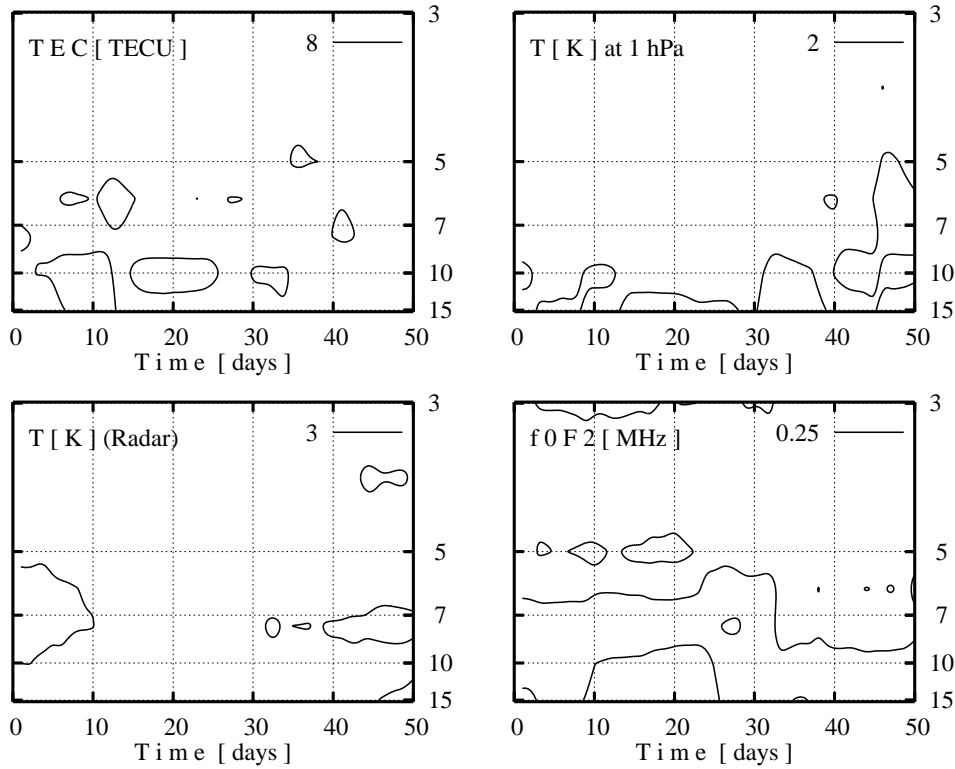


Figure 7: Spectral analysis of a 30 day running window starting on 1st September 2004. The 30 day time window is 50 times shifted forward by 1 day. The solid lines indicate wave activity dependent on time and the period of wave (y-axis).

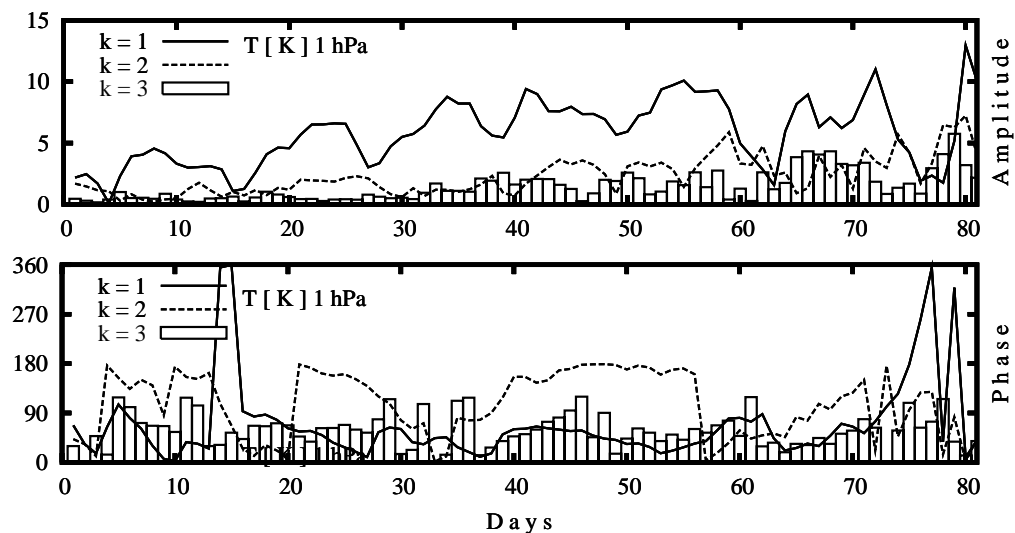


Figure 8: Time Series of the zonal harmonic analyzed amplitudes (upper panel) and phases (lower panel) of the wavenumbers $k=1$ (solid), 2 (dashed), 3 (boxes) dependent on time for temperature at 1.0 hPa and latitude $55^\circ N$.

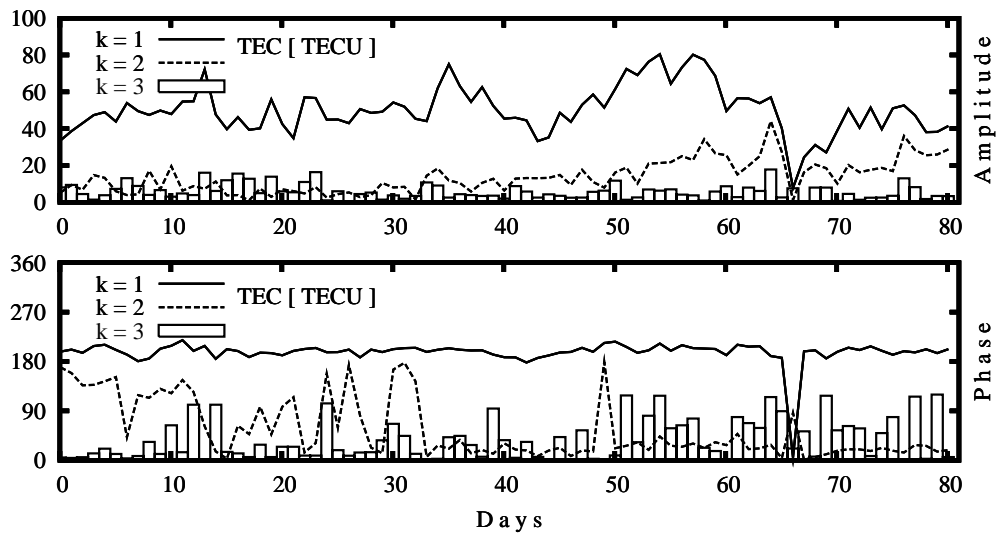


Figure 9: Time Series of the zonal harmonic analyzed amplitudes (upper panel) and phases (lower panel) of the wavenumbers $k=1$ (solid), 2 (dashed), 3 (boxes) dependent on time for TEC data at latitude $55^\circ N$.

Summary and conclusion

Planetary waves can propagate in time and space. Lawrence and Jarvis (2003) have observed planetary wave activity at quasi 16, 10 and 5 days period at various altitudes from 30 to 220 km and at mid-latitude. A permanent monitoring of the TEC on global scale using GPS satellites allows to study the meteorological influence on ionospheric variability and can help to create a climatology of planetary wave propagation up to the lower thermosphere. In this study we analysed long-periodic variations in autumn 2004 (1st September to 20th November) at a range of height between about 50 km and 300 km. The comparison with the analysis of the assimilated stratospheric UK Met Office data at 1.0 hPa height (temperature) as well as the meteor radar temperature at Collm ($51.3^\circ N$, $13.0^\circ E$) and the measured f_0F2 frequency of the ionosonde at Juliusruh ($54.6^\circ N$, $13.4^\circ E$) indicates similar structures. The spectral analysis of given atmospheric data shows a strong amplitude for variations near 30 days and a quasi 6 day signature in all data. In the analysed TEC data the quasi 16-day wave is not visible. There are also peaks near 9- and 12- days. A good correspondence exists between the radar temperature and f_0F2 frequency spectrum.

The global TEC and temperature data at 1.0 hPa height are spatially analysed followed by the spectral analysis of every zonal wavenumber $k=1, 2, 3$. The timeseries of the resulting amplitudes show a very dominant wavenumber 1 in global TEC data with an almost constant phase. The results of this first case study in analyzing global TEC-maps at mid-latitude region show signatures of planetary waves activity in ionospheric F-layer. In a next step, we calculate a time-space cross spectra (Hayashi, 1971) to classify types of planetary waves after zonal wavenumber, period and travelling direction along longitude. Future investigations study the mechanisms of planetary wave propagation into the lower thermosphere.

Acknowledgements

The GNSS TEC data are provided by DLR Neustrelitz, the ionosonde data by IAP Kühlungsborn and the meteor radar data by the University of Leipzig. The assimilated stratospheric data of UK Met Office are taken from the british atmospheric data center (BADC) server. Many thanks especially to K. Fröhlich for her first advises in analyzing stratospheric data, A. Pogoreltsev for some useful hints in separating planetary waves and M. Mudelsee for his careful correction reading.

The project is supported by DFG under grant JA 836/19-1.

References

- Altadill, D., Apostolov, E.M., Jacobi, C., Mitchell, N.J., 2003, Six-day westward propagating wave in the maximum electron density of the ionosphere, *Annales Geophysicae* 21, 1577-1588.
- Forbes, J. M., Palo, S. E., Zhang, X., 2000, Variability of the ionosphere, *J. Atmos. Solar-Terr. Phys.* 62, 685-693
- Hayashi, Y., 1971, A method of analyzing transient waves by space-time cross spectra, *J. App. Meteor.* 12, 404-408.
- Hocking, W. K., 1999, Temperature using radar-meteor decay times, *Geophys. Res. Lett.* 62, 3297-3300.
- Jacobi, Ch., Kürchner, D., Fröhlich, K., Arnold, K., Tetzlaff, G., 2005, Meteor radar wind and temperature measurements over Collm during autumn 2004, *Sci. Rep. Met. Inst. Univ. L.* 36, 98-112.
- Jakowski, N., Heise, S., Wehrenpfennig, A., Schlüter, S., Reimer, R., 2002, GPS/GLONASS-based TEC measurements as a contributor for space weather forecast, *J. Atmos. Solar-Terr. Phys.* 64, 729-735.
- Kohl, H., Rüster, R., Schlegel, K., 1996, Modern ionospheric science, *ProduServ GmbH Verlagsservice*, 371-390.
- Lastovicka, J., 2005, Forcing of the ionosphere by waves from below, *J. Atmos. Solar-Terr. Phys.*
- Lawrence, A. R., Jarvis, M. J., 2003, Simultaneous observations of planetary waves from 30 to 220 km, *J. Atmos. Solar-Terr. Phys.* 65, 765-777
- Lorenc, A., et al, 2000, The Met Office global 3-dimensional variational data assimilation scheme, *Quart. J. R. Meteorol. Soc.* 126, 2991-3012.
- Swinbank, R., O'Neill, A., 1994, A stratosphere-troposphere data assimilation system, *Monthly Weath. Rev.* 122, 686-702.